

Original research article

1
2
3
4
5
6
7
8
9
10
11
12
13
14
15
16

Targeting the Histone Methyltransferase SETD7 Rescues Diabetes-induced Impairment of Angiogenic Response by Transcriptional Repression of Semaphorin 3G

Shafeeq A. Mohammed, PhD¹, Era Gorica, PhD¹, Mattia Albiero, PhD^{2,3}, Gergely Karsai, PhD⁴, Alessandro Mengozzi, MD, PhD^{1,5,6}, Carlo Maria Caravaggi, MD⁷, Samuele Ambrosini, PhD¹, Stefano Masi, MD, PhD^{5,8}, Maria Cristina Vinci, PhD⁹, Gaia Spinetti, PhD¹⁰, Sanjay Rajagopalan, MD^{11,12}, Assam El-Osta, PhD^{13,14,15}, Jaroslav Pelisek¹⁶, Frank Ruschitzka, MD^{1,17}, Gian Paolo Fadini, MD, PhD^{2,3}, Sarah Costantino, PhD^{1,17§}, Francesco Paneni, MD, PhD^{1,17§*}

- ¹Center for Translational and Experimental Cardiology (CTEC), Department of Cardiology, Zurich University Hospital and University of Zürich, Wagistrasse 12, Schlieren CH-8952, Switzerland.
- ²Department of Surgery, Oncology and Gastroenterology - University of Padova, Italy.
- ³Veneto Institute of Molecular Medicine, Padova, Italy.
- ⁴Institute of Clinical Chemistry, University Hospital Zurich, University of Zurich, Zurich-8091, Switzerland.
- ⁵Department of Clinical and Experimental Medicine, University of Pisa, Pisa, Italy
- ⁶Health Science Interdisciplinary Center, Sant'Anna School of Advanced Studies, Pisa, Italy;
- ⁷Diabetic Foot Department, IRCCS MultiMedica, Milan, Italy.
- ⁸Institute of Cardiovascular Science, University College London, London, UK
- ⁹Unit of Vascular Biology and Regenerative Medicine, Centro Cardiologico Monzino IRCCS, 20138 Milan, Italy.
- ¹⁰Cardiovascular Pathophysiology-Regenerative Medicine Laboratory, IRCCS MultiMedica, Milan, Italy.
- ¹¹Harrington Heart and Vascular Institute, University Hospitals, Cleveland, OH.
- ¹²Case Western Reserve University School of Medicine, Cardiovascular Research Institute, Cleveland, OH.
- ¹³Baker Heart and Diabetes Institute, Epigenetics in Human Health and Disease Program, Melbourne, Vic, Australia;
- ¹⁴Department of Diabetes, Central Clinical School, Monash University, Melbourne, Vic, Australia;
- ¹⁵University College Copenhagen, Faculty of Health, Department of Technology, Biomedical Laboratory Science, Copenhagen, Denmark;
- ¹⁶Department of Vascular Surgery, University Hospital Zurich, 8091 Zurich, Switzerland;
- ¹⁷University Heart Center, Cardiology, University Hospital Zurich, Zürich, Switzerland.
- §The authors contributed equally to this work.

***Address for Correspondence:**

Prof. Dr. med. Francesco Paneni, FESC
Director, Center for Translational and Experimental Cardiology (CTEC)
Head, Cardiometabolic Division
University Heart Center
Department of Cardiology
Rämistrasse 100
CH-8091 Zürich
francesco.paneni@uzh.ch
www.herzzentrum.usz.ch

NOTE: This preprint reports new research that has not been certified by peer review and should not be used to guide clinical practice.

1 **Abstract**

2

3 **Background:** Peripheral artery disease (PAD) is highly prevalent in patients with diabetes
4 (DM) and associates with a poor prognosis. Revascularization strategies failed to improve
5 outcome, suggesting that new strategies to promote blood vessel growth are needed.
6 Histone modifications have emerged as key modulators of gene expression, however their
7 role in angiogenic response in DM remains poorly understood. Here we investigate the role
8 of chromatin remodelling in DM-related impairment of angiogenic response. **Methodology:**
9 Primary human aortic endothelial cells (HAECs) were exposed to normal glucose (NG, 5
10 mM) or high glucose (HG, 25 mM) for 48 hours. Gene expression profiling was performed by
11 RNA sequencing (RNA-seq). Cell migration and tube formation were employed to study
12 angiogenic properties in HAECs. Levels of the histone methyltransferase SETD7 and its
13 chromatin signature at histone 3 on lysine 4 (H3K4me1) were investigated by Western blot
14 and chromatin immunoprecipitation (ChIP). Pharmacological blockade of SETD7 was
15 achieved by using the selective inhibitor (*R*)-PFI-2 while the inactive enantiomer (*S*)-PFI-2
16 was used as a control. Mice with streptozotocin-induced DM were orally treated with (*R*)-PFI-
17 2 or vehicle and underwent hindlimb ischemia by femoral artery ligation. Our experimental
18 findings were translated in endothelial cells and gastrocnemius muscle samples obtained
19 from DM patients with PAD. **Results:** RNA-seq in HG-treated HAECs unveiled the histone
20 methyltransferase SETD7 as the top-ranking transcript. SETD7 upregulation was associated
21 with increased H3K4me1 levels as well as with impaired HAECs migration and tube
22 formation. Both SETD7 silencing and inhibition by (*R*)-PFI-2 rescued hyperglycemia-induced
23 impairment of HAECs migration and tube formation, while SETD7 overexpression blunted
24 the angiogenic response. RNA-seq and ChIP assays showed that SETD7-induced
25 H3K4me1 enables the transcription of the angiogenesis inhibitor semaphorin-3G (SEMA3G)
26 by increasing chromatin accessibility to PPAR γ . Moreover, SEMA3G overexpression
27 mimicked the impairment of angiogenic response observed during hyperglycemia. In DM
28 mice with hindlimb ischemia, (*R*)-PFI-2 improved limb perfusion by suppressing SEMA3G.
29 Finally, RNAseq and immunofluorescence in vascular specimens from two cohorts of DM
30 patients with PAD confirmed the upregulation of SETD7/SEMA3G signalling. Of note, (*R*)-
31 PFI-2 restored angiogenic properties in HAECs collected from DM patients. **Conclusion:**
32 SETD7 is a druggable epigenetic target to promote neovascularization in DM.

33

34

35

36

37

1 **Introduction**

2
3 Diabetes mellitus (DM) is a major cause of disability due to the occurrence of micro- and
4 macrovascular complications.¹ Among the constellation of cardiovascular comorbidities, DM
5 shows the highest association with peripheral artery disease (PAD), a condition
6 characterized by atherosclerotic lesions, reduced blood supply and chronic ischemia of the
7 lower extremities.² DM is highly prevalent in patients with PAD and has been co-diagnosed
8 in nearly 40% of all PAD patients.³ Despite advances in revascularization strategies, the rate
9 of limb amputation due to chronic limb ischemia remains high and associates with
10 cardiovascular morbidity in DM patients.³⁻⁵ In this perspective, strategies that promote
11 vascularization can be considered as a novel therapeutic option in DM patients with PAD.⁶⁻⁸
12 Epigenetic changes, defined as plastic chemical modifications of DNA/histone complexes –
13 have shown to modulate gene activity by modifying chromatin accessibility to transcription
14 factors.^{9, 10} To date, only few studies have investigated the contribution of epigenetic
15 modifications in regulating angiogenic response and post-ischemic vascularization.^{11, 12}
16 Inhibition of histone deacetylase 9 (HDAC9) was shown to impair endothelial cells (ECs)
17 tube formation, sprouting and retinal vessel outgrowth, whereas HDAC9 overexpression
18 rescued the impairment of angiogenesis.¹³ In another study, pharmacological inhibition and
19 genetic ablation of transcriptional co-activator p300-CBP associated factor (PCAF) impaired
20 blood flow recovery and arteriogenesis following hindlimb ischemia via suppression of
21 inflammatory signalling and leukocyte recruitment.¹⁴ Although these studies highlighted a
22 pivotal role of chromatin remodelling in the regulation of EC angiogenic properties, our
23 understanding of epigenetic regulation of angiogenic response in diabetes remains poor and
24 chromatin-editing approaches with specific epi-drugs are yet to be approved in this setting.
25 In the present study we show that, among chromatin modifying enzymes, the histone
26 methyltransferase SETD7 is strongly upregulated by hyperglycemia and impairs angiogenic
27 response by transcriptional regulation of the anti-angiogenic gene semaphorin3G
28 (SEMA3G). Pharmacological targeting of SETD7 by (*R*)PFI-2 was able to rescue DM-

1 induced impairment of angiogenic properties both *in vitro* and *in vivo*. Activation of the
2 SETD7/SEMA-3G axis was validated by RNA-seq and immunofluorescence in two different
3 cohorts of patients with DM and PAD. Notably, SETD7 inhibition by (R)PFI-2 rescued
4 migration and tube formation in ECs collected from DM patients thus suggesting the
5 potential clinical relevance of our study. Taken together, these findings suggest that
6 selective pharmacological blockade of SETD7 could help restoring post-ischemic
7 neovascularization thus preventing limb ischemia in DM.

8

9 **Methods**

10 An extended version of the methods used in this study is provided in Supplemental Material.

11 **Experiments in human aortic endothelial cells**

12 Human aortic endothelial cells (HAECs, passages 5 to 7) were cultured in EBM-2 (growth
13 factor-free medium) with 2% FBS and exposed for 48 hours either to normal glucose (5
14 mmol/L) or high glucose concentrations (25 mmol/L), in the presence or in the absence of
15 the SETD7 inhibitor R-PFI-2 (20 μ M) or its inactive enantiomer S-PFI-2 (20 μ M). Mannitol at
16 the final concentration of 20 mmol/L was used as an osmotic control. After 48 h cells were
17 harvested and used for angiogenesis assays or molecular analyses.

18 **RNA-sequencing**

19 RNA-sequencing (RNA-seq) was performed in NG and HG-treated HAECs, in the presence
20 or in the absence of SETD7-siRNA or scrambled siRNA (n=5/group). Samples were
21 sequenced as a75 bp paired end with a NextSeq 500 using the Truseq LT kit (please see
22 Supplemental Material for details about RNA-seq and bioinformatic analysis).

23 **Chromatin immunoprecipitation (ChIP) assays**

24 Chromatin immunoprecipitation was performed in HAECs and mouse gastrocnemius muscle
25 specimens by using the Magna ChIP Assay Kit (Millipore, Billerica, USA), according to the
26 manufacturer's instructions. ChIP quantifications of gene promoters were performed by real

1 time PCR (gene primers are shown in **Table S1**). Quantifications were performed using the
2 comparative cycle threshold method and are reported as the n fold difference in antibody-
3 bound chromatin against the input DNA, as previously reported.^{15, 16}

4 **Mouse model of diabetic hindlimb ischemia**

5 Diabetes was induced in 8-week-old male mice (C57BL/6) by a single high dose of
6 streptozotocin (STZ, 175 mg/Kg, via intraperitoneal injection) as previously reported.¹⁷ For
7 the hindlimb ischemia experiments, animals were sedated with 5% inhaled Isoflurane (Iso-
8 Vet, Piramal Healthcare, UK) and kept at 2-3% for maintenance. Analgesia was achieved
9 with 5 mg/kg tramadol. The femoral artery and the vein were surgically dissected from the
10 femoral nerve, then cauterized by applying an electric current with a bipolar tweezer end
11 excised from the proximal end to popliteal bifurcation. Hindlimb perfusion was measured with
12 Perimed PeriscanPim II Laser Doppler System (PerimedAB, Sweden) at 1, 7 and 14 days
13 after ischemia. Animal experiments were approved by the Veneto Institute of Molecular
14 Medicine Animal Care and Use Committee and by the Italian Health Ministry.

15 **In vivo treatment with (R)-PFI-2**

16 (R)-PFI-2 hydrochloride (Cat. HY-18627A, MedChemExpress) at the final dose of 95 mg/Kg
17 or vehicle (DMSO:Corneal oil at 1:1 ratio) were given orally in mice for 5 days before the
18 induction of hindlimb ischemia and continued for the next 14 days. Body weight and blood
19 glucose levels were monitored before and after treatment. At the end of the study, mice were
20 harvested, and liver specimens were tested for possible toxicity.

21 **RNA-seq in DM patients with PAD and healthy control donors**

22 Human vascular tissue samples were collected from DM patients with PAD who underwent
23 open surgical interventions at the Department of Vascular Surgery at the University Hospital
24 Zurich. Control aortas were obtained from healthy donors and provided by the Department of
25 Visceral Surgery at the University Hospital Zurich. The local ethics committee (Cantonal
26 Ethics Committee Zurich, Switzerland; BASEC-Nr. 2020-00378) approved the tissue sample

1 collection and processing for molecular analyses. The detailed methods for library
2 preparation and RNA-seq are reported in Supplemental Material.

3 **Collection of skeletal muscle specimens from DM patients with PAD**

4 Skeletal muscle specimens were obtained from a second cohort of DM patients with PAD to
5 validate our findings. The collection of human samples was approved by the MultiMedica
6 Research Ethics Committee and was conducted according to the principles outlined in the
7 Declaration of Helsinki. Specimens were collected from: i) different anatomical locations of
8 the lower extremities from non-diabetic control participants, referred for
9 investigations/therapeutic interventions related to leg varicosity; or ii) foot muscle from T2D
10 participants at the occasion of minor amputation for chronic limb ischemia (diagnosed
11 according to the Trans-Atlantic Inter-Society Consensus Document on Management of
12 Peripheral Arterial Disease [TASC].

13 **Experiments in primary endothelial cells collected from patients**

14 Primary human aortic endothelial cells (passages 5–7, Clonetics®) were obtained from DM
15 patients (M:F=2:2; age, 61±2 years; n=4), free from overt cardiovascular disease and other
16 relevant comorbidities. Cells were grown in fibronectin-coated 75 cm² flasks in optimized
17 endothelial growth medium-2 supplemented with 2% fetal bovine serum, as previously
18 described.¹⁸ Treatment with (*R*)-PFI-2 was performed as described above and in
19 Supplemental Material.

20

1 Results

2 **Hyperglycemia leads to an impairment of angiogenic response and SETD7** 3 **upregulation in human aortic endothelial cells (HAECs)**

4 To investigate whether HG may impact on angiogenesis *in vitro*, we exposed primary human
5 aortic endothelial cells (HAECs) to normal glucose (NG, 5 mM/L) and high glucose
6 concentrations (HG, 25 mM/L) for 24 and 48 hours. Compared with NG, HG led to an
7 impairment of endothelial migration, tube formation and sprouting (**Fig. 1A-C**). To unveil
8 transcriptional signatures potentially involved in hyperglycemia-induced impairment of
9 angiogenesis, we employed an unbiased approach by performing RNA-seq in HAECs treated
10 with NG and HG. Among dysregulated genes, HAECs treated with HG displayed a significant
11 upregulation of the histone methyltransferase SETD7 (**Fig. 1D-E; Fig. S1A**). Consistently with
12 this finding, HG led to a time-dependent increase in SETD7 gene expression and protein
13 levels (**Fig. 1F, Fig. S1B-C**), whereas no changes in SETD7 expression were observed with
14 the osmotic control mannitol (**Fig. S1D**). Since SETD7 is specifically involved in mono-
15 methylation of lysine 4 at histone 3 (H3K4me1)¹⁸⁻²⁰, we next investigated this chromatin
16 signature and found an increase in H3K4me1 levels in HG-treated HAECs as compared to the
17 NG group (**Fig. 1G**). In line with enhanced histone methylation, we observed an increased
18 nuclear translocation of SETD7 upon HG treatment, as shown by immunoblotting and
19 immunofluorescence (**Fig 1H-I, Fig. S2A-B**).

20 **SETD7 inhibition blunts H3K4me1 levels and rescues hyperglycemia-induced defects** 21 **of angiogenic response.**

22 We next investigated whether SETD7 inhibition could restore angiogenic response in HAECs
23 exposed to HG. Of interest, SETD7 depletion by small interfering RNA (siRNA) reduced
24 H3K4me1 levels while restoring EC migration and tube formation as compared to scrambled
25 siRNA (Scr.siRNA) (**Fig. 2A-C**). Given its specificity for H3K4me1, gene silencing of SETD7

1 did not affect other H3K4 methylation marks (H3K4me3) (**Fig. S3**). Next, we employed a
2 highly selective pharmacological inhibitor of SETD7, (*R*)-PFI-2, and used its inactive
3 enantiomer (*S*)-PFI-2 as a control. HAECs treated with (*R*)-PFI-2 showed neither signs of
4 cell toxicity nor changes in cell morphology (**Fig. S4A-B**). Consistent with the siRNA
5 experiments, (*R*)-PFI-2 treatment led to a reduction of H3K4me1 levels and associated with
6 an improvement of angiogenic properties (**Fig. 2D-F**). As expected, the drug did not affect
7 H3K4me3 levels (**Fig. S4C**).

8 **SEMA3G is a downstream target of SETD7**

9 We next performed RNA-seq in HG-treated HAECs with and without SETD7 depletion to
10 appraise SETD7-dependent transcriptional changes in ECs (**Fig. 3A**). SETD7 knockdown in
11 HAECs was associated with significant changes in the expression of genes implicated in the
12 regulation of vasculogenesis, angiogenesis and cell migration (as shown by IPA analysis,
13 **Fig. 3B**). Specifically, SETD7-depleted HAECs displayed a significant downregulation of
14 SEMA3G, VCAM1, PTGS1 and DUSP23 (**Fig. 3C, Fig. S5**). In order to unveil SETD7
15 transcriptional targets, we interrogated the UCSC genome browser
16 (<https://genome.ucsc.edu>) to investigate the enrichment of SETD7-specific histone marks
17 (H3K4me1) on the promoter of deregulated genes (**Fig. 3D**). SEMA3G promoter showed a
18 strong enrichment in H3K4me1, suggesting a potential involvement of SETD7 in its
19 transcriptional regulation (**Fig. 3D**). SEMA3G was significantly upregulated upon HG
20 exposure as compared to NG (**S6A-B**), while SETD7 gene silencing in HG-treated HAECs
21 led to a significant downregulation of SEMA3G levels as compared to Scr.siRNA, suggesting
22 that SETD7 is required for SEMA3G upregulation (**Fig. 3E, S6A-B**). A similar downregulation
23 of SEMA3G was observed with the selective SETD7 inhibitor (*R*)-PFI-2 as compared to its
24 inactive enantiomer (*S*)-PFI-2 (**Fig. 3F**). On the other hand, SETD7 overexpression in NG-
25 treated HAECs was sufficient to increase SEMA3G protein levels and mimicked
26 hyperglycemia-induced impairment of ECs migration and tube formation (**Fig. 3G-I**).

1
2
3
4
5
6
7
8
9
10
11
12
13
14
15
16
17
18
19
20
21
22
23
24
25
26
27
28

SEMA3G is preferentially expressed in aortic endothelial cells and represses angiogenic capacity

In order to explore the expression pattern of SEMA3G in the vascular endothelium, we analyzed a single-cell RNAseq dataset previously generated in mouse skeletal muscle specimens.²¹ scRNA-seq profiles were obtained from 4,121 cells with a median of 959 genes per cell. Unsupervised clustering followed by t-distributed stochastic neighbor embedding (t-SNE) revealed six clusters of vascular ECs, which all expressed the pan-vascular markers *Cdh5* and *Pecam1* while did not express described marker sets of muscle stem cells and other muscle cell types.²¹ Of interest, we found that SEMA3G was preferentially enriched in aortic endothelial cells and arteriole endothelial cells (**Fig. 4A**). To characterize the function of SEMA3G in the diabetic endothelium we performed loss-of-function experiments by siRNA. We observed that SEMA3G silencing in HG-treated HAECs restored cell migration and tube formation (**Fig. 4B-C**).

SETD7 regulates SEMA3G secretion in endothelial cells

Recent work has shown that SEMA3G can be secreted from cells.²² Hence, we investigated whether SETD7 inhibition could affect SEMA3G secretion from cultured HAECs exposed to HG. SEMA3G secretion was enhanced in HG-treated HAECs as compared to NG, whereas treatment with the SETD7 inhibitor (*R*)-PFI-2 significantly reduced SEMA3G levels in conditioned media as compared to its inactive enantiomer (*S*)-PFI-2 (**Fig. 4D**).

SETD7-dependent H3K4me1 favors chromatin accessibility on SEMA3G promoter

To appraise whether SETD7 regulates SEMA3G via H3K4me1 (transcriptional mechanism) rather than by direct protein methylation (posttranslational mechanism), we performed co-immunoprecipitation to test a direct interaction between SETD7 and SEMA3G. No interaction between the 2 proteins was observed upon HG exposure (**Fig. S7**). Bioinformatic analysis of ChIP-seq data from the UCSC genome browser showed a strong enrichment of

1 H3K4me1 on SEMA3G promoter (**Fig. 5A**). To confirm these data, we performed a ChIP
2 assay by leveraging three sets of primers targeting different regions of SEMA3G promoter
3 (**Fig. 5B**). ChIP assay performed in HG-treated HAECs revealed that H3K4me1 is
4 preferentially enriched at the initiator site of SEMA3G promoter (**Fig. S8A**). Interestingly
5 enough, H3K4me1 enrichment on SEMA3G promoter was reduced in the presence of (*R*-
6 PFI-2 in HG-treated HAECs, as compared to (*S*)-PFI-2 (**Fig. 5C**). Moreover, SETD7
7 inhibition only affected H3K4me1 but not H3K4me3 enrichment, in line with the notion that
8 SETD7 specifically induces histone mono-methylation (**Fig. S8B**). This set of data shows
9 that SETD7-induced H3K4me1 is required for SEMA3G transcription.

10 **PPAR γ drives SEMA3G transcription**

11 *In silico* analysis showed that both PPAR γ and SOX18 could potentially act as transcription
12 factors on the SEMA3G promoter (**Fig. 5D**). By leveraging motif binding analysis
13 (<https://jaspar.genereg.net/>) we next determined the nucleotide sequence of transcription
14 factor binding site (**Fig. 5E**). ChIP assay revealed a strong binding of the transcription factor
15 PPAR γ to SEMA3G promoter, while no binding was observed for SOX18 (**Fig. 5F**). These
16 results were confirmed by experiments with siRNA-mediated depletion of both PPAR γ and
17 SOX18 showing a reduction of SEMA3G expression and protein levels only in presence of
18 PPAR γ but not SOX18-siRNA (**Fig. 5G-H, Fig. S9A-B**). PPAR γ -siRNA did not affect SETD7
19 protein levels (**Fig. S9C**). To further validate the role of PPAR γ in SEMA3G transcription, we
20 treated HAECs with the PPAR γ agonist pioglitazone. Notably, HAECs treated with
21 pioglitazone showed increased SEMA3G expression and protein levels as compared to
22 vehicle (**Fig. 5I, Fig. S10A-B**). Pioglitazone did not affect SETD7 expression (**Fig. S10B-C**).

23 **(*R*)-PFI-2 improves post-ischemic vascularization and limb perfusion in diabetic mice**

24 Prompted by our *in vitro* results, we next determined whether SETD7 inhibition could rescue
25 ischemia-mediated angiogenesis *in vivo*, in a model of diabetic hindlimb ischemia. Diabetes
26 was induced by streptozotocin while control mice received citrate buffer alone, as previously

1 reported.¹⁷ After 4 weeks, subgroups of diabetic and non-diabetic mice were randomized to
2 oral treatment with (*R*)-PFI-2 (95 mg/kg/day) or vehicle 6 days before the induction of
3 hindlimb ischemia till 14 days following limb ischemia, for a total of 20 days. Alanine
4 transaminase (ALT) assay excluded liver toxicity in mice treated with (*R*)-PFI-2 (**Fig. S11A**).
5 Diabetes led to increased blood glucose levels and body weight loss as compared to non-
6 diabetic mice, and these alterations were not affected by (*R*)-PFI-2 treatment (**Fig. S11B-C**).
7 Following hindlimb ischemia, diabetic mice exhibited a marked impairment of blood perfusion
8 as assessed by laser Doppler Imaging (blood flow of ischemic vs. non-ischemic hindlimb at
9 14 days (0.48 ± 0.02 vs 0.36 ± 0.02 , $p = 0.003$) as compared to non-diabetic controls
10 (**Fig.6A-B**). Treatment with (*R*)-PFI-2 restored blood perfusion levels in diabetic mice as
11 compared to vehicle (0.36 ± 0.02 vs 0.51 ± 0.04 , $p=0.025$) (**Fig. 6A-B**). The observed
12 improvement of limb perfusion with (*R*)-PFI-2 was associated with restoration of capillary
13 density, as shown by CD31 immunofluorescence in cross-sections from gastrocnemius
14 muscles of diabetic mice (**Fig. 6D**).

15

16 **In vivo modulation of SETD7/SEMA3G axis by (*R*)-PFI-2**

17 In line with our *in vitro* data, SETD7/SEMA3G axis was dysregulated in ischemic
18 gastrocnemius muscles from diabetic as compared to non-diabetic mice, as shown by real
19 time PCR and Western blot (**Fig. 6E, Fig. S12**). (*R*)-PFI-2 treatment suppressed
20 SETD7/SEMA3G expression while decreasing H3K4me1 levels (**Fig. 6E, Fig. S12**).
21 Mechanistically, ChIP assays showed that (*R*)-PFI-2 prevented the enrichment of both
22 H3K4me1 and the transcription factor PPAR γ on SEMA3G promoter (**Fig. 6F-G**). Of interest,
23 we found that *in vivo* treatment with (*R*)-PFI-2 reduced plasma levels of SEMA3G in diabetic
24 mice (**Fig. 6H**).

1 **SETD7/SEMA3G signaling in diabetic patients with PAD**

2 To translate our experimental findings to humans, we first performed RNA-seq in vascular
3 specimens collected from DM patients with PAD undergoing elective surgical
4 revascularization and age-matched healthy controls. Of note, RNA-seq confirmed a
5 significant dysregulation of both SETD7 and SEMA3G (**Fig. 7A**). SETD7/SEMA3G axis and
6 H3K4me1 expression were then validated in a second cohort of patients, where
7 gastrocnemius muscle specimens were collected from non-diabetic patients (controls) and
8 age-matched patients with DM and PAD. Immunofluorescence confirmed the upregulation of
9 SETD7, SEMA3G and H3K4me1 in DM patients as compared to controls (**Fig.7B-C**).
10 Pearson's correlation confirmed the nuclear translocation of SETD7 in muscular specimens
11 from DM patients as compared to controls (**Fig. 7D**). Real-time PCR confirmed SETD7 and
12 SEMA3G upregulation in DM patients with PAD (**Fig. 7E**). Interestingly, ChIP assay
13 confirmed the enrichment of PPAR γ and H3K4me1 on SEMA3G promoter in muscle
14 specimens from DM patients with PAD as compared to controls (**Fig. 7F-G**).

15 **Targeting SETD7 restores angiogenic properties in the human diabetic endothelium**

16 We next investigated whether pharmacological modulation of SETD7 in the human diabetic
17 endothelium could rescue angiogenic properties. To this end, we employed human aortic
18 endothelial cells isolated from patients with DM (M:F=2:2; age, 61 \pm 2 years; n=4). (*R*)-PFI-2
19 attenuated SEMA3G expression and H4K3me1 levels in diabetic ECs as compared to its
20 inactive enantiomer (*S*)-PFI-2 (**Fig. 8A-B**). Moreover, SETD7 inhibition significantly improved
21 EC cell migration and tube formation (**Fig. 8C-D**). A schematic summarizing the main study
22 findings is reported in **Fig. 8E**.

23

24 **Discussion**

25

1 In the present study we show that, among different genes deregulated by hyperglycemia, the
2 histone methyltransferase SETD7 is a pivotal chromatin remodeler fostering transcriptional
3 programs leading to defective angiogenesis and reduced limb perfusion in diabetic mice.
4 The most important findings of our study are: i) RNA-seq in human aortic endothelial cells
5 exposed to hyperglycemia unveiled SETD7 as the top-ranking transcript; ii) hyperglycemia
6 increases SETD7 expression and SETD7-dependent H3K4me1, thus leading to an open
7 chromatin and active transcription of the anti-angiogenic gene SEMA3G; iii) Both gene
8 silencing and selective pharmacological inhibition of SETD7 by (*R*)-PFI-2 blunt H3K4me1
9 levels and SEMA3G transcription thus rescuing hyperglycemia-induced impairment of
10 angiogenic properties; iv) in diabetic mice, the SETD7 inhibitor (*R*)-PFI-2 rescues post-
11 ischemic vascularization and limb perfusion by suppressing SEMA3G transcription; (v)
12 SETD7/SEMA3G signalling was dysregulated in two different cohorts of DM patients with
13 PAD; iv) treatment with (*R*)-PFI-2 in ECs collected from DM patients restored angiogenic
14 properties.

15 Over the last few years, an increasing body of evidence showed that epigenetic changes
16 affect transcriptional programs implicated in blood vessel growth and angiogenic response.²³
17 The growing understanding of chromatin structure has led to the design of specific drugs
18 with ability to erase or write epigenetic signatures eventually resetting the cell transcriptome
19 in disease states.²⁰ Notably, several of these compounds have been already approved by
20 the FDA for the treatment of cancer, neurological and autoimmune diseases.²⁴ Post-
21 translational modifications of histone tails, namely acetylation and methylation, induce
22 chromatin remodelling that may either enable or repress gene transcription.¹⁰ *In vitro* studies
23 have recently shown that SETD7 is involved in epigenetic regulation of the transcription
24 factor NF- κ B.^{25, 26} In addition, SETD7 induces MCP-1 upregulation and endoplasmic
25 reticulum stress in the kidney of diabetic mice.²⁷ Although these studies provide important
26 mechanistic insights on the role of SETD7 in hyperglycemia-induced inflammation, SETD7
27 function in the vascular endothelium remains poorly understood.

1 In the present study, we show for the first time that SETD7 is a pivotal repressor of blood
2 vessel growth in the setting of diabetic PAD. Specifically, in conditions of hyperglycaemia
3 SETD7 monomethylates H3K4me1 in proximity of SEMA3G promoter. These chromatin
4 signatures enables changes in chromatin accessibility ultimately favouring SEMA3G
5 transcription and subsequent impairment of EC migration and tube formation. This was
6 demonstrated by SETD7 gain- and loss-of-function approaches. SETD7 overexpression
7 mimicked defective angiogenesis while its depletion or pharmacological blockade by (*R*)-
8 PFI-2 rescued hyperglycaemia-induced impairment of angiogenic properties. We showed
9 that SETD7-dependent histone mono-methylation was causally involved in SEMA3G
10 upregulation. First, co-immunoprecipitation experiments ruled out a direct protein
11 methylation of SEMA3G by SETD7. Furthermore, SETD7 is the only methyl-writing enzyme
12 responsible for H3K4me1¹⁹ and this confers specificity to our findings. Indeed, we did not
13 observe any change of other H4K4 methylation sites (i.e.H3K4me3) following SETD7
14 manipulation. However, H3K4me1 is amenable to demethylation by the lysine-specific
15 demethylase 1 (LSD1)^{26, 28} and further experiments should elucidate the fine balance and
16 interplay between SETD7 and LSD1 in the regulation of SEMA3G transcription. An active
17 downregulation of LSD1 could also participate to enhanced H3K4me1 levels in our study.
18 Although histone methylation is emerging as a pivotal determinant of transcriptional and
19 phenotypic changes in different cell types^{29, 30}, methylation of non-histone proteins by SETD7
20 may also play a role in endothelial homeostasis. For example, SETD7-dependent
21 methylation and LSD1-dependent demethylation of hypoxia-inducible factor-1 α (HIF-1 α)
22 were recently reported to regulate protein stability in the nucleus in a proline hydroxylation-
23 and VHL-independent manner during normoxic and hypoxic conditions.³¹ We cannot exclude
24 that non-histone methylation by SETD7 could participate to the observed changes in
25 angiogenic properties, and that other SETD7 targets could be involved in the setting of DM..
26 An interesting aspect of our study is that, once transcribed, SEMA3G is secreted by
27 endothelial cells, and this process is regulated by SETD7. Indeed, both SETD7 depletion by
28 siRNA and pharmacological blockade by (*R*)-PFI-2 were able to blunt SEMA3G levels in

1 conditioned media from cultured human endothelial cells. Of note, circulating levels of
2 SEMA3G were increased in diabetic mice with hindlimb ischemia, while *in vivo* treatment
3 with (*R*)-PFI-2 led to a significant reduction of SEMA3G levels in plasma. Hence, SETD7
4 inhibition could prevent detrimental actions of SEMA3G in target organs. In this regard, a
5 recent study showed that SEMA3G promotes adipocyte differentiation, adipogenesis and
6 insulin resistance while its inhibition prevented metabolic alterations in mice.³² Moreover,
7 SEMA3G plasma levels were increased in obese patients and positively correlated with
8 circulating leptin and adipokines levels.³² Hence, SETD7 inhibition could contribute to
9 prevent SEMA3G-dependent metabolic alterations thus broadening the potential applicability
10 of our findings. Furthermore, our results indicate that SEMA3G could represent a potential
11 biomarker of defective angiogenesis, and future studies should explore this possibility.

12 In our work, we identified PPAR γ as the transcription factor responsible for SEMA3G
13 transcription. CHIP experiments confirmed PPAR γ binding to SEMA3G promoter while
14 PPAR γ depletion prevented SEMA3G transcription in HAECs. These findings were further
15 confirmed by treatment with the PPAR γ agonist pioglitazone which was sufficient to induce
16 SEMA3G transcription. These data could also help to understand the results of clinical trials
17 where pioglitazone was associated with increased hazard for surgical or percutaneous lower
18 extremity revascularization in patients with DM.³³ In line with our findings, a previous study
19 showed that *in vivo* treatment with pioglitazone was associated with decreased ischemic
20 limb perfusion and capillary density in a rat model of hindlimb ischemia.³⁴ Hence,
21 pioglitazone-induced SEMA3G could be a plausible mechanistic explanation for the
22 observed impairment of limb perfusion with this drug.

23 Consistent with our *in vitro* observations, *in vivo* inhibition of SETD7 by (*R*)-PFI-2 was able to
24 restore limb perfusion and capillary density in diabetic mice with hindlimb ischemia. At the
25 molecular level, we showed that oral administration of (*R*)-PFI-2 was associated with blunted
26 H3K4me1 levels as well as reduced SEMA3G transcription and secretion in plasma. The
27 SETD7 pharmacological inhibitor (*R*)-PFI-2 was recently reported as a first-in-class, potent
28 (Kiapp = 0.33 nM), selective, and cell-active inhibitor of the SETD7 methyltransferase

1 activity.^{35, 36} Our results in diabetic mice pave the way for translational studies testing the
2 effects of SETD7 inhibitors in preclinical models of PAD and limb ischemia. To appraise
3 whether our experimental findings hold true in the human setting, we further investigated
4 SETD7/SEMA3G signalling in two different cohorts of diabetic patients. RNA-seq and
5 immunofluorescence confirmed the upregulation of SETD7/SEMA3G axis in diabetic patients
6 with PAD as compared to healthy controls. Furthermore, we showed a significant enrichment
7 of H3K4me1 on SEMA3G promoter in patient samples, suggesting that (R)-PFI-2 might
8 represent a promising therapeutic intervention in this clinical setting. Of clinical relevance,
9 (R)-PFI-2 restored angiogenic properties in ECs obtained from DM patients, suggesting the
10 possibility of a therapeutic modulation of SETD7 in DM patients. The lack of toxicity and
11 adverse effects associated with (R)-PFI-2 treatment in mice supports the plausibility of
12 testing (R)-PFI-2 in a pre-clinical and clinical setting.

13 Our study has some limitations. Although hyperglycemia was able to induce a significant
14 upregulation of SETD7, the mechanistic link between high glucose and increased SETD7
15 activity remains to be elucidated. The N-terminal region of SETD7 contains membrane
16 occupation and recognition nexus (MORN) motifs, which are known to be involved in stress
17 response and regulation of SETD7 localization.³⁷ Further experiments should elucidate the
18 role of MORN motifs as a potential mechanism linking cellular stress to SETD7 localization
19 and activity in our setting. Furthermore, the role of other cells potentially involved in the in
20 vivo improvement of limb perfusion and capillary density was not addressed in this study.
21 Although we show an important function of SETD7 in endothelial cells, other relevant cell
22 types, namely pericytes and immune cells, could contribute to the observed phenotype.

23 In conclusion, our translational study unveils a druggable target to boost post-ischemic
24 vascularization in the setting of diabetes. Our results pave the way for preclinical studies in
25 larger animal models to better define the potential of SETD7-targeting approaches in DM
26 patients with PAD and limb ischemia.

27

28 **Sources of Funding**

1 This work was supported by the Swiss National Science Foundation (n. 310030_197557),
2 the Swiss Heart Foundation (n. FF19045), the Olga Mayenfisch Foundation, the Swiss Life
3 Foundation, the Kurt und Senta-Hermann Stiftung, the EMDO Stiftung, the Schweizerische
4 Diabetes-Stiftung, the Novo Nordisk Foundation and the Novartis Foundation for Biomedical
5 Research (to F.P.); the Holcim Foundation and the Swiss Heart Foundation (to SC); the
6 Italian Ministry of Health (Ricerca Corrente to the IRCCS MultiMedica).

7

8

9 **Disclosures**

10 There are no competing interests related to the present work. F.P. is a consultant to Vectura
11 Fertin Pharma and has received personal fees for lectures from Novo Nordisk.

12

13 **Figure legends**

14 **Figure 1. Defective angiogenesis and upregulation of the histone methyltransferase**
15 **SETD7 by hyperglycemia.** HAECs were cultured in growth factor-free medium and
16 exposed to normal glucose concentrations (NG, 5 mM/L) or high glucose concentration (HG,
17 25 mM/L) for 24 and 48 hours. **A)** Scratch assay and relative quantification showing
18 migration of HAECs exposed to NG and HG; **B)** Representative images of Matrigel-based
19 tube formation assay in the 2 experimental groups. For quantification, the length of tubule
20 (yellow arrow) and loop (LO) formation were considered; **C)** Endothelial sprouting and
21 relative quantification in aortic rings from non-diabetic and diabetic mice; **D-E)** Heatmap and
22 volcano plot displaying differential gene expression in HAECs exposed to NG vs HG; (fold
23 change 2 to -2; significantly downregulated genes are shown in green while upregulated
24 genes are shown in red); **F)** Representative Western blot and relative quantification showing
25 SETD7 protein levels in HAECs treated with NG and HG at different time points (6, 12, 24
26 and 48 hours). GAPDH and Vinculin were used as loading controls; **G)** Representative
27 Western blot and relative quantification showing H3K4me1 levels in HAECs treated with NG
28 and HG at different time points (6, 12, 24 and 48 hours). Histone 3 was used as a loading
29 control; **H)** Representative Western blot and relative quantification showing SETD7
30 localization in cytosolic and nuclear fractions from HAECs treated with NG and HG; **I)**
31 Immunostaining and Pearson's coefficient showing the localization of SETD7 in HAECs
32 treated with NG and HG. Nuclei are shown in blue (DAPI), whereas SETD7 is shown in

1 green. Data are expressed as mean \pm SD and shown as a percentage of control. Multiple
2 comparisons were performed by one-way ANOVA followed by Bonferroni post hoc test
3 where appropriate. A p value <0.05 was considered significant. HG, high glucose; NG,
4 normal glucose.

5 **Figure 2. SETD7 inhibition reduces H3K4me1 levels while rescuing HG-induced**
6 **defects of angiogenic response.** **A)** Representative Western blot and relative
7 quantification showing SETD7 and H3K4me1 levels in HAECs treated with HG, in presence
8 of SETD7-siRNA and scramble-siRNA. GAPDH and histone 3 were used as loading
9 controls; **B)** Scratch assay and relative quantification showing migration of HG-treated
10 HAECs in presence of SETD7-siRNA and scramble-siRNA; **C)** Representative images of
11 Matrigel-based tube formation assay in the different experimental groups. For quantification,
12 the length of tubule (indicated by arrow) and loop (LO) formation was considered; **D)**
13 Representative Western blot and relative quantification showing H3K4me1 levels in HAECs
14 treated with HG, in the presence of the SETD7-selective inhibitor (*R*)-PFI-2 and its inactive
15 enantiomer (*S*)-PFI-2. Histone 3 was used as a loading control; **E-F)** Scratch assay and
16 Matrigel-based tube formation assay in HG-treated HAECs treated with (*R*)-PFI-2 or (*S*)-PFI-
17 2. Data are expressed as mean \pm SD and shown as a percentage of control. Comparisons
18 were performed by Student's t test. A p value <0.05 was considered significant.

19 **Figure 3. The angiogenesis inhibitor SEMA3G is a downstream target of SETD7.** **A)**
20 Heatmap showing differential gene expression in HG-treated HAECs, in the presence of
21 SETD7-siRNA or Scr.siRNA (fold change 2 to -2; downregulated genes are shown in green
22 while upregulated transcripts are shown in red); **B)** IPA (Ingenuity Pathway Analysis)
23 displaying signaling pathways affected by SETD7 depletion; **C)** Volcano plot shows
24 differential gene expression in HG-treated HAECs with and without SETD7 depletion by
25 siRNA (fold change 2 to -2; downregulated genes are shown in green while upregulated
26 transcripts are shown in red); **D)** UCSC genome analysis showing enrichment of different
27 histone marks on gene promoters; **E)** Representative Western blot and relative quantification
28 of SEMA3G in HAECs treated with HG+SETD7 siRNA vs. HG+ Scr.siRNA; **F)**
29 Representative Western blot and relative quantification of SEMA3G in HG-treated HAECs, in
30 presence of the SETD7-selective inhibitor (*R*)-PFI-2 or its inactive enantiomer (*S*)-PFI-2; **G)**
31 Representative Western blot and relative quantification of SEMA3G expression following
32 SETD7 overexpression in HAECs. A scrambled genomic RNA (Scr.Grna) was used as
33 control for SETD7 overexpression; **H)** Scratch assay and relative quantification showing
34 migration of HG-treated HAECs in presence of SETD7 overexpression or Scr.Grna (control);
35 **I)** Representative images of Matrigel-based tube formation assay in the different

1 experimental groups. Multiple comparisons were performed by one-way ANOVA followed by
2 Bonferroni post hoc test where appropriate. A p value <0.05 was considered significant.

3 **Figure 4. SEMA3G is preferentially expressed in aortic endothelial cells and represses**
4 **angiogenic capacity. A)** Bioinformatic analysis of scRNA-seq data obtained in skeletal
5 muscle-derived endothelial cells (<https://shiny.debocklab.hest.ethz.ch/Fan-et-al/>). Violin plots
6 show normalized SEMA3G expression in each EC cluster; **B)** Scratch assay and relative
7 quantification showing migration of HG-treated HAECs in presence of SEMA3G-siRNA and
8 scr.siRNA; **C)** Representative images of Matrigel-based tube formation assay in the different
9 experimental groups; **D)** ELISA showing SEMA3G levels in conditioned media from HAECs
10 treated with NG and HG, in presence of SETD7-selective inhibitor (R)-PFI-2 and its inactive
11 enantiomer (S)-PFI-2. Multiple comparisons were performed by one-way ANOVA followed
12 by Bonferroni post-hoc test where appropriate. A p value <0.05 was considered significant.

13 **Figure 5. PPAR γ regulates SEMA3G transcription. A)** Analysis of ChIP-seq data
14 (available from the UCSC genome browser) showing enrichment of chromatin marks
15 (H3K4me1, H3K27ac) on SEMA3G promoter; **B)** Schematic showing ChIP primers targeting
16 three different regions of SEMA3G promoter; **C)** ChIP assay showing enrichment of
17 H3K4me1 on SEMA3G promoter in HG-treated HAECs; **D)** *In silico* prediction analysis
18 shows PPAR γ and SOX18 as transcription factors potentially involved in SEMA3G
19 transcription; **E)** Motif binding analysis (JASPAR) showing the sequence for transcription
20 binding site; **F)** ChIP assay showing enrichment of PPAR γ and SOX-18 on SEMA3G
21 promoter. Chromatin was immunoprecipitated with normal rabbit IgG or antibody against
22 SOX-18 and PPAR γ , and precipitated genomic DNA was analyzed by real-time PCR using
23 primers for SEMA3G promoter; n = 4/group; **G)** Representative Western blot and relative
24 quantification of SEMA3G and PPAR γ in HG-treated HAECs, in presence of PPAR γ siRNA
25 or Scr.siRNA; **H)** Representative Western blot and relative quantification of SEMA3G and
26 SOX18 in HG-treated HAECs with and without SOX18 depletion; **I)** Representative Western
27 blot and relative quantification of SEMA3G and PPAR γ expression in HAECs treated with
28 the PPAR γ agonist pioglitazone or vehicle (DMSO). Multiple comparisons were performed
29 by one-way ANOVA followed by Bonferroni post-hoc test where appropriate. A p value <0.05
30 was considered significant.

31 **Fig.6. SETD7 inhibition by (R)-PFI-2 improves post-ischemic vascularization and limb**
32 **perfusion in diabetic mice**

33 Unilateral hindlimb ischemia was surgically induced in non-diabetic and diabetic C57BL/6J
34 male mice; **A)** Laser Doppler perfusion imaging was serially performed to determine blood
35 flow recovery at 24 h, 7 and 14 days after hindlimb ischemia; **B)** Time-dependent changes of

1 blood flow recovery (expressed as the ratio of blood perfusion in the
2 ischemic versus nonischemic hind limb) in diabetic and non-diabetic mice treated with (*R*)-
3 PFI-2 or vehicle; *, $p < 0.05$; **C**) Immunostaining (CD31) and relative quantification showing
4 capillary density in gastrocnemius muscle samples. Scale bar = 50 μm ; $n = 9/\text{group}$; **D**) Real-
5 time PCR showing gene expression of SETD7 and SEMA3G in gastrocnemius muscle
6 obtained from non-diabetic and diabetic mice treated with vehicle or (*R*)-PFI-2; **E**)
7 Representative Western blot of SETD7, SEMA3G and H3K4me1 in gastrocnemius muscle
8 obtained from non-diabetic mice and diabetic mice treated with vehicle or (*R*)-PFI-2. GAPDH
9 and histone 3 were used as loading controls; **F-G**) ChIP assay showing enrichment of
10 PPARG and H3K4me1 on SEMA3G promoter. Chromatin was immunoprecipitated with
11 normal rabbit IgG or antibody against PPARG and H3K4me1, and precipitated genomic DNA
12 was analyzed by real-time PCR using primers for SEMA3G promoter, $n = 4/\text{group}$. **H**)
13 Circulating SEMA3G levels in plasma samples from diabetic mice treated with (*R*)-PFI-2 or
14 vehicle. Data are expressed as mean \pm SD and shown as a percentage of control. Multiple
15 comparisons were performed by one-way ANOVA followed by Bonferroni correction and
16 Student's t-test where appropriate. A p value < 0.05 was considered significant.

17 **Fig.7. Dysregulation of SETD7/SEMA3G signaling in patients with DM and PAD. A)**
18 RNA-seq data show the upregulation of SETD7 and SEMA3G gene expression in vascular
19 specimens from DM patients with PAD as compared to healthy controls; **B-C**).
20 Immunofluorescence and relative quantification showing SETD7, SEMA3G and H3K4me1
21 expression in lower limb muscle specimens from healthy and DM patients with PAD; **D**)
22 Representative immunofluorescence images showing localization of SETD7 in lower limb
23 muscle specimens from DM patients with PAD and non-diabetic controls. SETD7 displays a
24 cytosolic localization in non-diabetic patients while it shows nuclear translocation in DM
25 patients with PAD. Nuclei were stained with DAPI (blue). Quantification of SETD7 nuclear
26 translocation was performed by using the Pearson's coefficient; **E**) Real-time PCR
27 confirming the upregulation of SEMA3G and SETD7 in muscular specimens from DM
28 patients with PAD versus non-diabetic controls; **F-G**) ChIP assay showing enrichment of
29 H3K4me1 and PPARG on SEMA3G promoter in muscular specimens from DM patients with
30 PAD versus non-diabetic controls. Chromatin was immunoprecipitated with normal rabbit
31 IgG or antibody against PPARG and H3K4me1, and precipitated genomic DNA was analyzed
32 by real-time PCR using primer of SEMA3G promoter. Data are expressed as mean \pm SD and
33 shown as a percentage of control. Multiple comparisons were performed by one-way
34 ANOVA followed by Bonferroni correction and Student's t-test where appropriate. A p value
35 < 0.05 was considered significant. * $p < 0.05$; ** $p < 0.01$; and *** $p < 0.001$. PAD, peripheral
36 artery disease; T2D, type 2 diabetes.

1 **Fig. 8. (R)-PFI-2 restores angiogenic properties in the human diabetic endothelium. A-**
2 **B)** (R)-PFI-2 attenuates SEMA3G expression and H4K3me1 levels in human aortic
3 endothelial cells isolated from patients with DM (D-HAECs). The inactive enantiomer (S)-
4 PFI-2 was used as a negative control; **C-D)** Cell migration and tube formation in D-HAECs
5 treated with (R)-PFI-2 and (S)-PFI-2. Comparisons were performed by Student's t-test where
6 appropriate. A p value <0.05 was considered significant; **E)** Schematic showing the role of
7 SETD7/SEMA3G axis and the effects of its therapeutic modulation to restore vascularization
8 in diabetic PAD.
9

1

2 **Abbreviations**

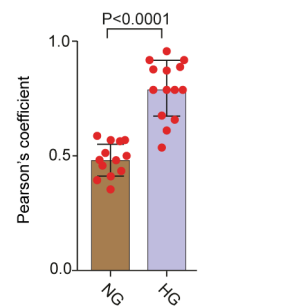
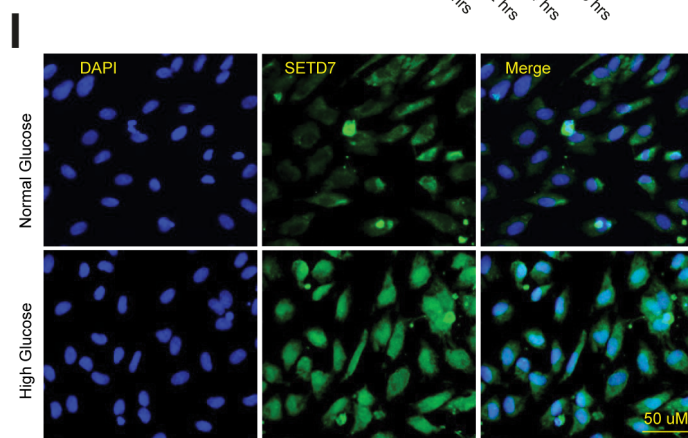
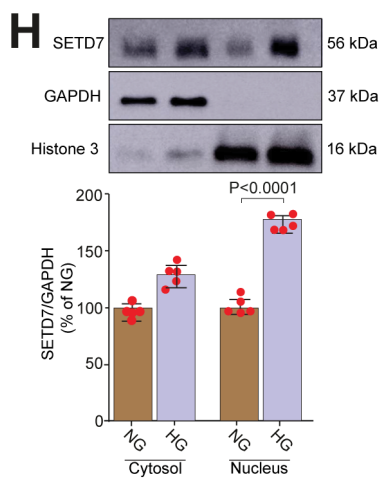
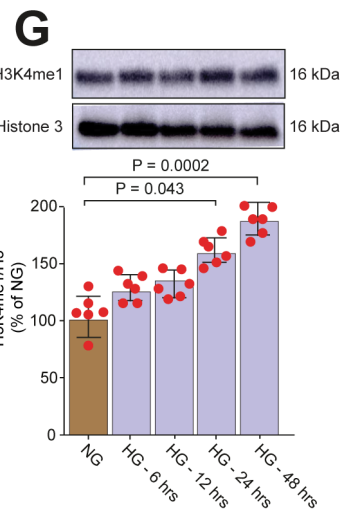
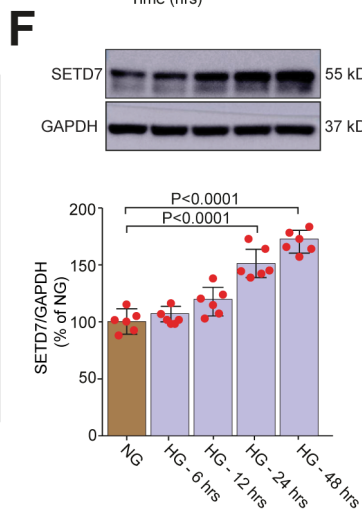
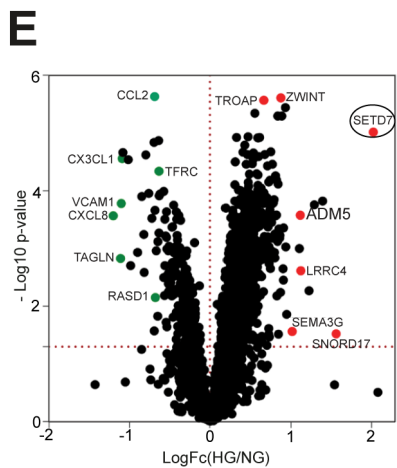
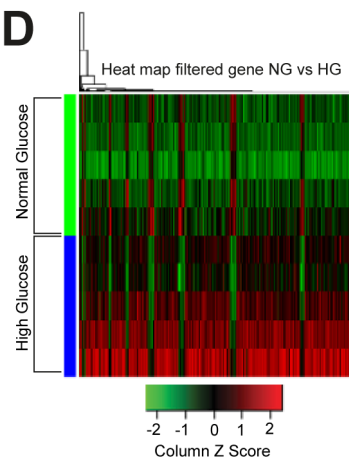
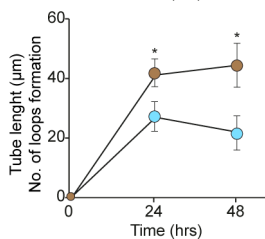
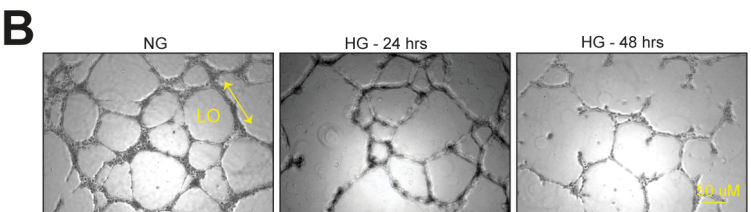
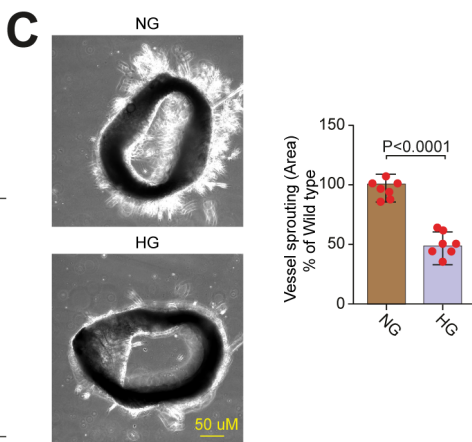
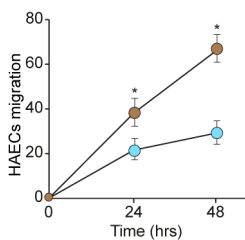
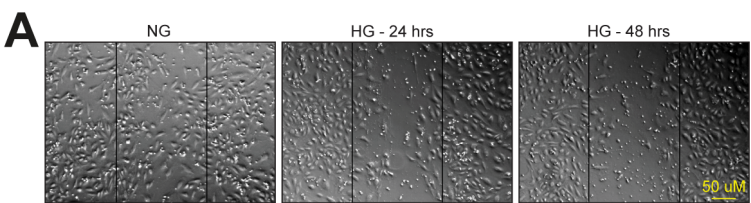
- 3 PAD: Peripheral artery disease
4 CLI: Critical limb ischemia
5 DM: Diabetes mellitus
6 CAD: Coronary artery disease
7 EC: Endothelial cell
8 HAECs: Human aortic endothelial cells
9 NG: Normal Glucose
10 HG: High Glucose
11 ChIP: Chromatin immunoprecipitation
12 VEGF: Vascular endothelial growth factor
13 H3k27ac: Histone 3 lysine 27 acetylation
14 MMT: 3-(4,5-dimethylthiazol-2-yl)-2,5-diphenyltetrazolium bromide
15 PCR: Polymerase chain reaction
16 SDS: sodium dodecyl sulfate
17 siRNA: small interfering RNA
18 GAPDH: Glyceraldehyde 3-phosphosphate dehydrogenase
19 STZ: streptozotocin
20 T2D: type 2 diabetes
21 TBP: TATA-Box binding protein
22 ChIP: Chromatin immunoprecipitation
23 ANOVA: analysis of variance
24 FDR: False discovery rate

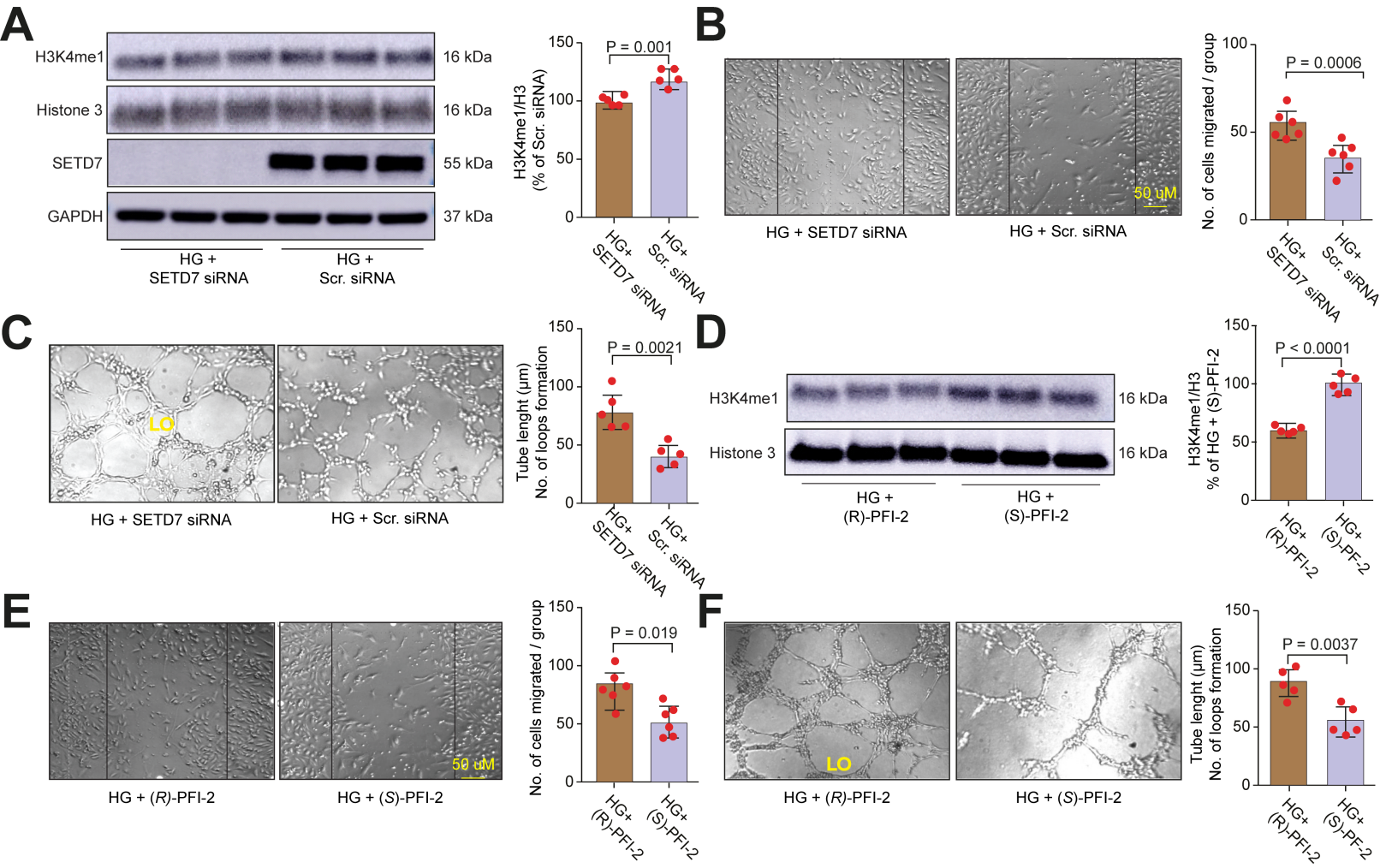
References

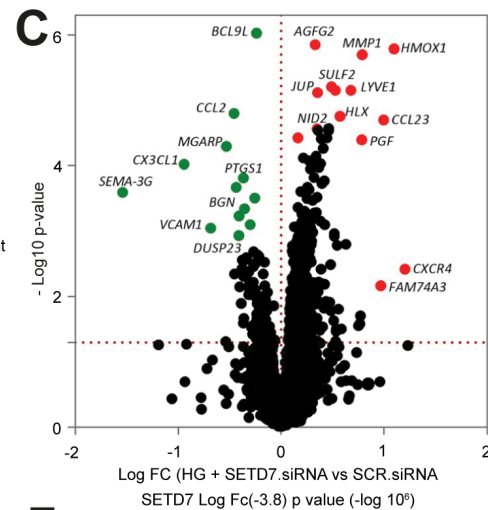
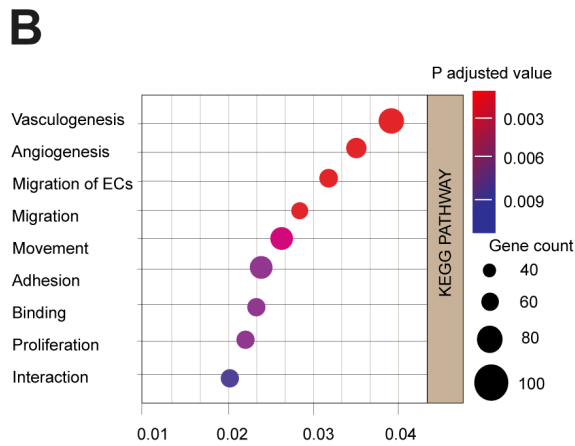
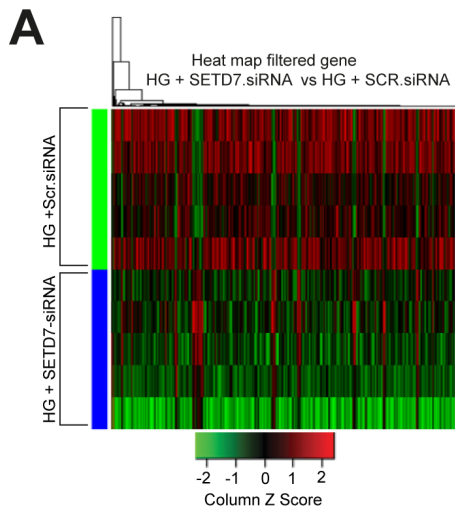
1. Lopez-Diez R, Egana-Gorrone L, Senatus L, Shekhtman A, Ramasamy R and Schmidt AM. Diabetes and Cardiovascular Complications: The Epidemics Continue. *Curr Cardiol Rep.* 2021;23:74.
2. Singh MV and Dokun AO. Diabetes mellitus in peripheral artery disease: Beyond a risk factor. *Front Cardiovasc Med.* 2023;10:1148040.
3. Barnes JA, Eid MA, Creager MA and Goodney PP. Epidemiology and Risk of Amputation in Patients With Diabetes Mellitus and Peripheral Artery Disease. *Arterioscler Thromb Vasc Biol.* 2020;40:1808-1817.
4. Humphries MD, Brunson A, Li CS, Melnikow J and Romano PS. Amputation trends for patients with lower extremity ulcers due to diabetes and peripheral artery disease using statewide data. *J Vasc Surg.* 2016;64:1747-1755 e3.
5. Mohammedi K, Woodward M, Hirakawa Y, Zoungas S, Colagiuri S, Hamet P, Harrap S, Poulter N, Matthews DR, Marre M, Chalmers J and Group AC. Presentations of major peripheral arterial disease and risk of major outcomes in patients with type 2 diabetes: results from the ADVANCE-ON study. *Cardiovasc Diabetol.* 2016;15:129.
6. Han J, Luo L, Marcelina O, Kasim V and Wu S. Therapeutic angiogenesis-based strategy for peripheral artery disease. *Theranostics.* 2022;12:5015-5033.
7. Caporali A, Back M, Daemen MJ, Hoefler IE, Jones EA, Lutgens E, Matter CM, Bochaton-Piallat ML, Siekmann AF, Sluimer JC, Steffens S, Tunon J, Vindis C, Wentzel JJ, Yla-Herttuala S and Evans PC. Future directions for therapeutic strategies in post-ischaemic vascularization: a position paper from European Society of Cardiology Working Group on Atherosclerosis and Vascular Biology. *Cardiovasc Res.* 2018;114:1411-1421.
8. Fadini GP, Spinetti G, Santopaolo M and Madeddu P. Impaired Regeneration Contributes to Poor Outcomes in Diabetic Peripheral Artery Disease. *Arterioscler Thromb Vasc Biol.* 2020;40:34-44.
9. Costantino S, Libby P, Kishore R, Tardif JC, El-Osta A and Paneni F. Epigenetics and precision medicine in cardiovascular patients: from basic concepts to the clinical arena. *Eur Heart J.* 2018;39:4150-4158.
10. Handy DE, Castro R and Loscalzo J. Epigenetic modifications: basic mechanisms and role in cardiovascular disease. *Circulation.* 2011;123:2145-56.
11. Fork C, Gu L, Hitzel J, Josipovic I, Hu J, SzeKa Wong M, Ponomareva Y, Albert M, Schmitz SU, Uchida S, Fleming I, Helin K, Steinhilber D, Leisegang MS and Brandes RP. Epigenetic Regulation of Angiogenesis by JARID1B-Induced Repression of HOXA5. *Arterioscler Thromb Vasc Biol.* 2015;35:1645-52.
12. Mitic T, Caporali A, Floris I, Meloni M, Marchetti M, Urrutia R, Angelini GD and Emanuelli C. EZH2 modulates angiogenesis in vitro and in a mouse model of limb ischemia. *Mol Ther.* 2015;23:32-42.
13. Kaluza D, Kroll J, Gesierich S, Manavski Y, Boeckel JN, Doebele C, Zelent A, Rossig L, Zeiher AM, Augustin HG, Urbich C and Dimmeler S. Histone deacetylase 9 promotes angiogenesis by targeting the antiangiogenic microRNA-17-92 cluster in endothelial cells. *Arterioscler Thromb Vasc Biol.* 2013;33:533-43.
14. Bastiaansen AJ, Ewing MM, de Boer HC, van der Pouw Kraan TC, de Vries MR, Peters EA, Welten SM, Arens R, Moore SM, Faber JE, Jukema JW, Hamming JF, Nossent AY and Quax PH. Lysine acetyltransferase PCAF is a key regulator of arteriogenesis. *Arterioscler Thromb Vasc Biol.* 2013;33:1902-10.
15. Costantino S, Paneni F, Virdis A, Hussain S, Mohammed SA, Capretti G, Akhmedov A, Dalgaard K, Chiandotto S, Pospisilik JA, Jenuwein T, Giorgio M, Volpe M, Taddei S, Luscher TF and Cosentino F. Interplay among H3K9-editing enzymes SUV39H1, JMJD2C and SRC-1 drives p66Shc transcription and vascular oxidative stress in obesity. *Eur Heart J.* 2019;40:383-391.

16. Costantino S, Akhmedov A, Melina G, Mohammed SA, Othman A, Ambrosini S, Wijnen WJ, Sada L, Ciavarella GM, Liberale L, Tanner FC, Matter CM, Hornemann T, Volpe M, Mechta-Grigoriou F, Camici GG, Sinatra R, Luscher TF and Paneni F. Obesity-induced activation of JunD promotes myocardial lipid accumulation and metabolic cardiomyopathy. *Eur Heart J*. 2019;40:997-1008.
17. Mohammed SA, Albiero M, Ambrosini S, Gorica E, Karsai G, Caravaggi CM, Masi S, Camici GG, Wenzl F, Calderone V, Madeddu P, Sciarretta S, Matter CM, Spinetti G, Luscher TF, Ruschitzka F, Costantino S, Fadini GP and Paneni F. The BET Protein Inhibitor Apabetalone Rescues Diabetes-induced Impairment of Angiogenic Response by Epigenetic Regulation of Thrombospondin-1. *Antioxid Redox Signal*. 2021.
18. Paneni F, Costantino S, Battista R, Castello L, Capretti G, Chiandotto S, Scavone G, Villano A, Pitocco D, Lanza G, Volpe M, Luscher TF and Cosentino F. Adverse epigenetic signatures by histone methyltransferase Set7 contribute to vascular dysfunction in patients with type 2 diabetes mellitus. *Circ Cardiovasc Genet*. 2015;8:150-8.
19. Okabe J, Orłowski C, Balcerczyk A, Tikellis C, Thomas MC, Cooper ME and El-Osta A. Distinguishing hyperglycemic changes by Set7 in vascular endothelial cells. *Circ Res*. 2012;110:1067-76.
20. Keating ST and El-Osta A. Epigenetics and metabolism. *Circ Res*. 2015;116:715-36.
21. Fan Z, Turiel G, Ardicoglu R, Ghobrial M, Masschelein E, Kocijan T, Zhang J, Tan G, Fitzgerald G, Gorski T, Alvarado-Diaz A, Gilardoni P, Adams CM, Ghesquiere B and De Bock K. Exercise-induced angiogenesis is dependent on metabolically primed ATF3/4(+) endothelial cells. *Cell Metab*. 2021;33:1793-1807 e9.
22. Liu X, Uemura A, Fukushima Y, Yoshida Y and Hirashima M. Semaphorin 3G Provides a Repulsive Guidance Cue to Lymphatic Endothelial Cells via Neuropilin-2/PlexinD1. *Cell Rep*. 2016;17:2299-2311.
23. Heuslein JL, Gorick CM and Price RJ. Epigenetic regulators of the revascularization response to chronic arterial occlusion. *Cardiovasc Res*. 2019;115:701-712.
24. Berdasco M and Esteller M. Clinical epigenetics: seizing opportunities for translation. *Nat Rev Genet*. 2019;20:109-127.
25. El-Osta A, Brasacchio D, Yao D, Poci A, Jones PL, Roeder RG, Cooper ME and Brownlee M. Transient high glucose causes persistent epigenetic changes and altered gene expression during subsequent normoglycemia. *J Exp Med*. 2008;205:2409-17.
26. Brasacchio D, Okabe J, Tikellis C, Balcerczyk A, George P, Baker EK, Calkin AC, Brownlee M, Cooper ME and El-Osta A. Hyperglycemia induces a dynamic cooperativity of histone methylase and demethylase enzymes associated with gene-activating epigenetic marks that coexist on the lysine tail. *Diabetes*. 2009;58:1229-36.
27. Chen J, Guo Y, Zeng W, Huang L, Pang Q, Nie L, Mu J, Yuan F and Feng B. ER stress triggers MCP-1 expression through SET7/9-induced histone methylation in the kidneys of db/db mice. *Am J Physiol Renal Physiol*. 2014;306:F916-25.
28. Reddy MA, Villeneuve LM, Wang M, Lanting L and Natarajan R. Role of the lysine-specific demethylase 1 in the proinflammatory phenotype of vascular smooth muscle cells of diabetic mice. *Circ Res*. 2008;103:615-23.
29. Mathiyalagan P, Keating ST, Du XJ and El-Osta A. Chromatin modifications remodel cardiac gene expression. *Cardiovasc Res*. 2014;103:7-16.
30. Gillette TG and Hill JA. Readers, writers, and erasers: chromatin as the whiteboard of heart disease. *Circ Res*. 2015;116:1245-53.
31. Kim Y, Nam HJ, Lee J, Park DY, Kim C, Yu YS, Kim D, Park SW, Bhin J, Hwang D, Lee H, Koh GY and Baek SH. Methylation-dependent regulation of HIF-1 α stability restricts retinal and tumour angiogenesis. *Nat Commun*. 2016;7:10347.
32. Liu M, Xie S, Liu W, Li J, Li C, Huang W, Li H, Song J and Zhang H. Mechanism of SEMA3G knockdown-mediated attenuation of high-fat diet-induced obesity. *J Endocrinol*. 2020;244:223-236.
33. Dormandy JA, Betteridge DJ, Schernthaner G, Pirags V, Norgren L and investigators PR. Impact of peripheral arterial disease in patients with diabetes--results from PROactive (PROactive 11). *Atherosclerosis*. 2009;202:272-81.

34. Dromparis P, Sutendra G, Paulin R, Proctor S, Michelakis ED and McMurtry MS. Pioglitazone inhibits HIF-1alpha-dependent angiogenesis in rats by paracrine and direct effects on endothelial cells. *J Mol Med (Berl)*. 2014;92:497-507.
35. Barsyte-Lovejoy D, Li F, Oudhoff MJ, Tatlock JH, Dong A, Zeng H, Wu H, Freeman SA, Schapira M, Senisterra GA, Kuznetsova E, Marcellus R, Allali-Hassani A, Kennedy S, Lambert JP, Couzens AL, Aman A, Gingras AC, Al-Awar R, Fish PV, Gerstenberger BS, Roberts L, Benn CL, Grimley RL, Braam MJ, Rossi FM, Sudol M, Brown PJ, Bunnage ME, Owen DR, Zaph C, Vedadi M and Arrowsmith CH. (R)-PFI-2 is a potent and selective inhibitor of SETD7 methyltransferase activity in cells. *Proc Natl Acad Sci U S A*. 2014;111:12853-8.
36. Ambrosini S, Montecucco F, Koliijn D, Pedicino D, Akhmedov A, Mohammed SA, Herwig M, Gorica E, Szabo PL, Weber L, Russo G, Vinci R, Matter CM, Liuzzo G, Brown PJ, Rossi FMV, Camici GG, Sciarretta S, Beltrami AP, Crea F, Podesser B, Luscher TF, Kiss A, Ruschitzka F, Hamdani N, Costantino S and Paneni F. Methylation of the Hippo effector YAP by the methyltransferase SETD7 drives myocardial ischaemic injury: a translational study. *Cardiovasc Res*. 2023;118:3374-3385.
37. Chiang C, Yang H, Zhu L, Chen C, Chen C, Zuo Y and Zheng D. The Epigenetic Regulation of Nonhistone Proteins by SETD7: New Targets in Cancer. *Front Genet*. 2022;13:918509.



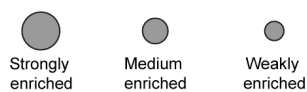




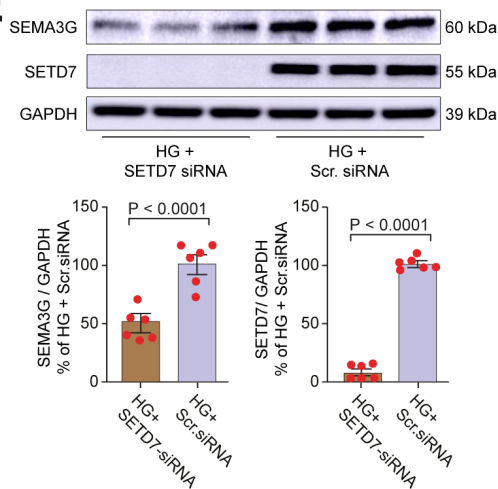
D

UCSC Genome analysis

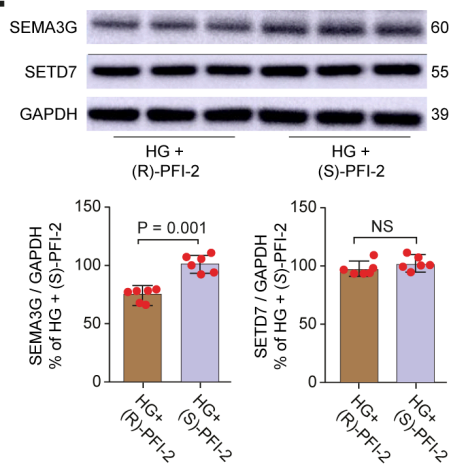
Genes	H3K27ac	H3K4me1	H3K4me3	Gene Site (hg38)
VCAM1	●	●	●	Chr1: 100,719,742
SEMA3G	●	●	●	Chr3: 52,433,035
PTGS1	●	●	●	Chr9: 52,433,035
DUSP23	●	●	●	Chr1: 159,780,932



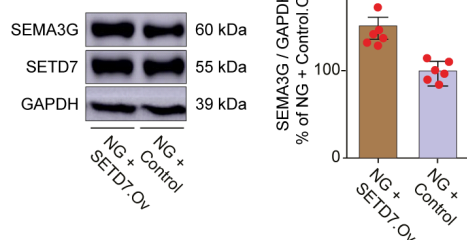
E



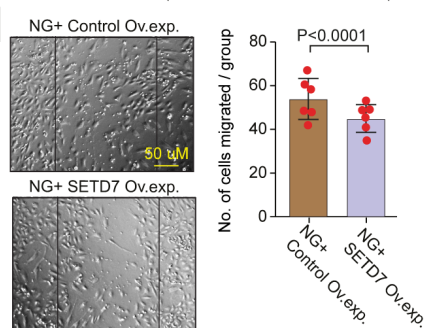
F



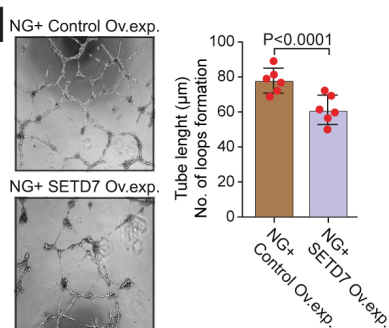
G

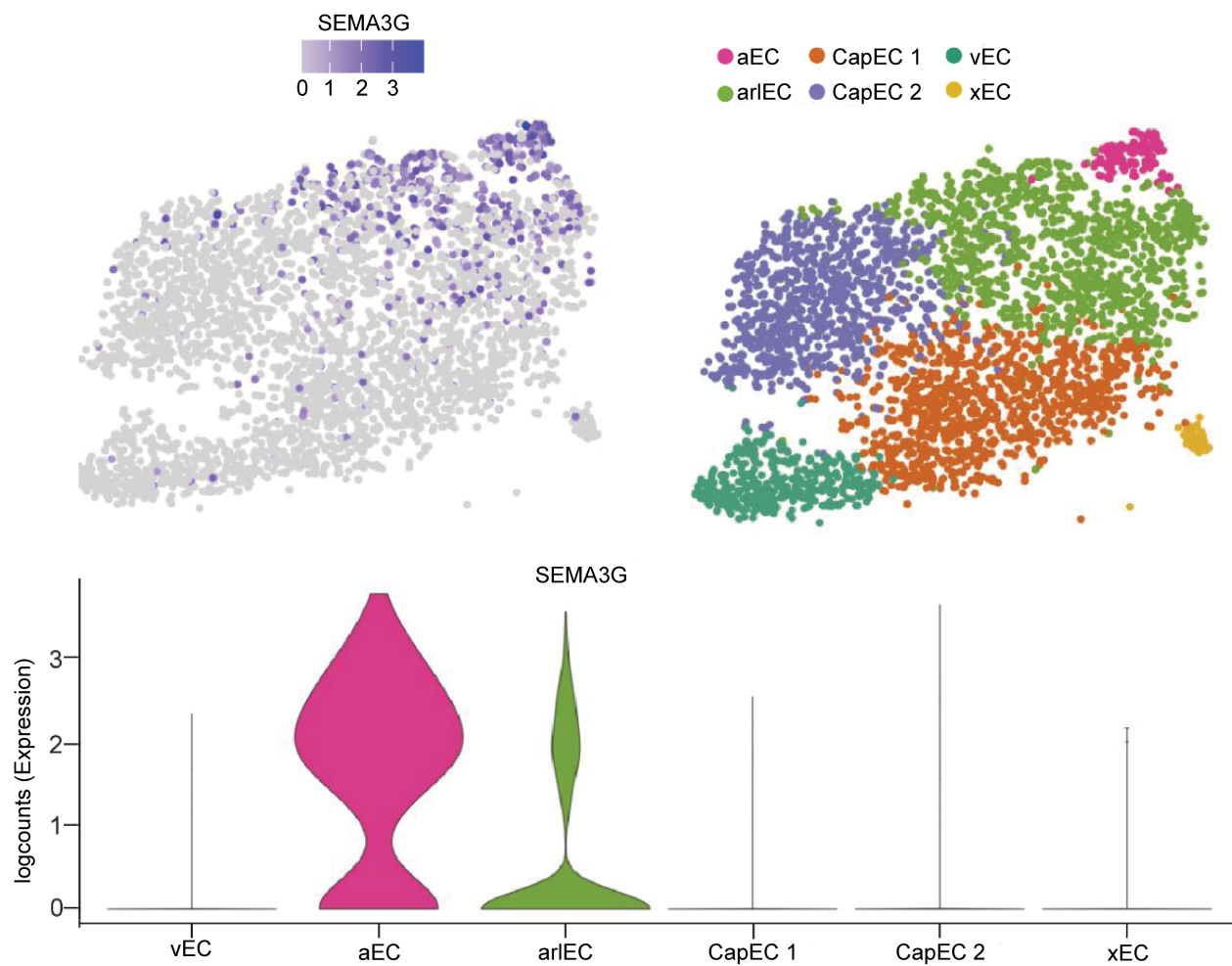
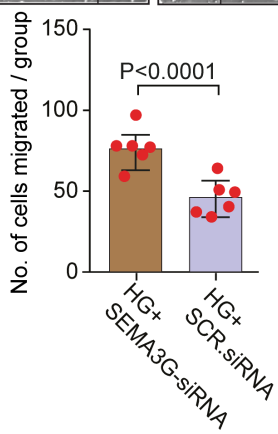
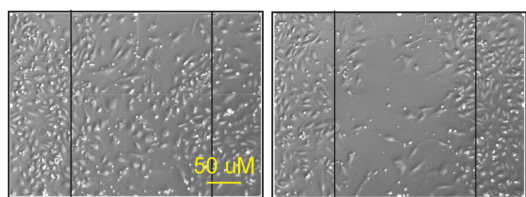
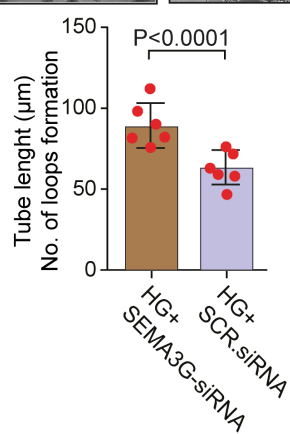
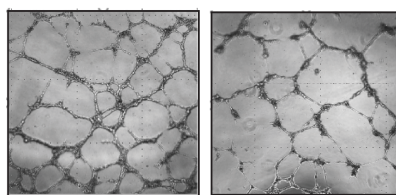


H



I



A**B****C****D**